

Quality assessment of high resolution wind and temperature observation from ModeS

revised edition

Siebren de Haan

De Bilt, 2010
(First published 2009)

PO Box 201
3730 AE De Bilt
Wilhelminalaan 10
De Bilt
The Netherlands
<http://www.knmi.nl>
Telephone +31(0)30-220 69 11
Telefax +31(0)30-221 04 07

Author: Haan, S. de

This revised edition presents the correction to figures 5.3, 5.4, 5.5 and 5.6.

Executive Summary

Wind, temperature and humidity observations from radiosonde and aircraft are the main sources of upper air information for meteorology. For meso-scale meteorology, the horizontal coverage of radiosondes is too sparse and aircraft observations through AMDAR (Aircraft Meteorological Data Relay) are insufficient because not all aircraft are equipped with an AMDAR system.

Observations inferred from an enhanced tracking and ranging (TAR) radar of Schiphol airport can fill this gap. This radar follows all aircraft in the airspace visible to the radar with a radius of 270km around the Netherlands for air-traffic management. This ModeS-radar contacts each aircraft every four seconds on which the transponder in the aircraft responds with a message that contains information on flight level, direction and speed. Together with the ground track of an aircraft, meteorological information on temperature and wind can be inferred from this information. Because all aircraft are required to respond to the TAR-radar, the data volume is extremely large, being around 1.5 million observations per day.

The quality of these observations is assessed by comparison to a numerical weather prediction (NWP) model information, AMDAR observations and radiosonde observations. A method to improve the temperature and wind observations is applied to enhance the quality wind and temperature observations, albeit with a reduced time frequency of one observation of horizontal wind vector and temperature per aircraft per minute. Nevertheless, the number of observations per day is still very large.

The temperature observations from ModeS, even after corrections are not very good; an RMS which twice as large as AMDAR is observed when compared to NWP. The quality found for wind after correction and calibration is good; it is comparable to AMDAR, slightly worse than radiosonde but certainly very valuable for NWP.

December 2009

Revision

Due to an error in the estimation of the wind direction from the NWP model, a deviation between zero to six degrees in wind direction from true north is observed. The error is caused by misinterpreting the NWP grid. The data used in Figures **5.3**, **5.4**, **5.5** and **5.6** are re-processed with the correct NWP wind.

February 2010

Contents

1	Introduction	1
1.1	Outline	2
2	Data	3
2.1	ModeS	3
2.2	AMDAR	4
2.3	Radiosonde	4
2.4	Numerical Weather Prediction	6
3	Meteorological Observations from Aircraft	7
3.1	Observations of Temperature and Wind	7
3.2	Air density and airspeed	8
3.3	Quality control	9
4	Preprocessing ModeS Observations	11
4.1	Preprocessing ModeS Temperature Observations	11
4.2	Preprocessing Wind Observations	14
4.2.1	Magnetic Heading correction	14
4.2.2	Heading Correction	14
5	Validation of ModeS	19
5.1	Triple comparison AMDAR, ModeS and NWP	19
5.2	Comparison Radiosonde, ModeS and NWP	21
5.3	Triple collation of ModeS, NWP and Radiosonde	25
6	Conclusions	29
	Bibliography	30

Chapter 1

Introduction

The major requirement of observational data for Numerical Weather Prediction (NWP) is upper air information of temperature, humidity and wind. The main sources of this information come from observations from radiosonde and aircraft. Radiosonde are generally launched two to four times a day, with land stations dominating this observations type. The radiosonde do not measure the wind vector, however by tracking the balloon during its ascent, wind information is inferred from the horizontal path. Radiosonde also measure humidity and the upper air observations from radiosondes are considered accurate.

Aircraft can measure wind and temperature by exploiting the on-board sensors. Designated AMDAR (Aircraft Meteorological Data Relay) aircraft have software installed which generate meteorological messages and sends these to the meteorological community through ground stations (e.g. located at aerodromes). An advantage of AMDAR is that the coverage includes data sparse areas such as over the oceans. However, intercontinental flights are using almost the same routes, leaving some areas un-sample. Moreover, these long-haul flights will provide observations at high flight levels only (approximately at 10 km altitude). AMDAR observations have a slightly worse quality than radiosonde; the measurement uncertainty of AMDAR temperature is approximately 1K (Drüe et al., 2007). In Ballish and Kumar (2008) it was shown that temperature observation from AMDAR exhibit a considerable variation with aircraft model and are on average warmer then radiosondes. Furthermore, Drüe et al. (2007) showed that systematic deviations in AMDAR wind measurements can be regarded as an error vector, which is fixed to the aircraft reference system. They found systematic deviations in wind measurements from different aircraft types (more than 0.5 m/s) parallel to parallel to the flight direction.

In this report a novel data source of upper air temperature and wind information is investigated. This data stems from the same source as AMDAR, but is collected in a different way by using the tracking and ranging radar at the airport of destination (Schiphol Airport). Aircrafts send out information on heading, airspeed and flight level for air-traffic control. This information is collected for all aircraft in view of the radar. Meteorological parameters, such as wind and temperature, can be deduced from this information comparable to AMDAR. The major difference with AMDAR is that information from all aircraft are gathered, in contrast to AMDAR where only dedicated aircraft equipped with AMDAR software can be used. Fur-

thermore, there are no costs for a data link. The messages are available and are received operationally for air-traffic management with a frequency of every four seconds. The coverage and observation frequency will be beneficial for (meso-scale) NWP and nowcasting when these observations have sufficient quality.

In this report, the quality of the these very high frequency observations is assessed by comparison with the NWP model HIRLAM (High Resolution Limited Area Model) run operationally at KNMI (Koninklijk Nederlands Meteorologisch Instituut), AMDAR and radiosonde observations.

1.1 Outline

This report is organized as follows: first the data used is described. Secondly, the method of inferring temperature and wind from aircraft is explained. Thirdly, correction algorithms used to improve the quality of the temperature and wind observations are presented. Comparison with AMDAR, NWP and radiosonde are described subsequently. We end with conclusions and recommendations.

Chapter 2

Data

2.1 ModeS

ModeS data is collected using the tracking and ranging radar (TAR-1) at Amsterdam Schiphol (EHAM) airport. On request by the radar, in response each individual aircraft sends information on the current speed and heading, from which temperature and wind can be inferred. The radar performs a full scan every four seconds and the area covered is 270 km around the radar. The coverage is limited by the curvature of the earth. The recorded messages contain information generated by the flight computer including the transponder-id, flight level, Mach-number, roll, true airspeed and heading. The message is complemented with information on the position and ground track from the tracking radar. All aircraft are queried, resulting in about $1.5 \cdot 10^6$ observations per day around Amsterdam Schiphol. Figure 2.1 shows the observations on 2008-03-13 between 11:00 UTC and 13:00 UTC.

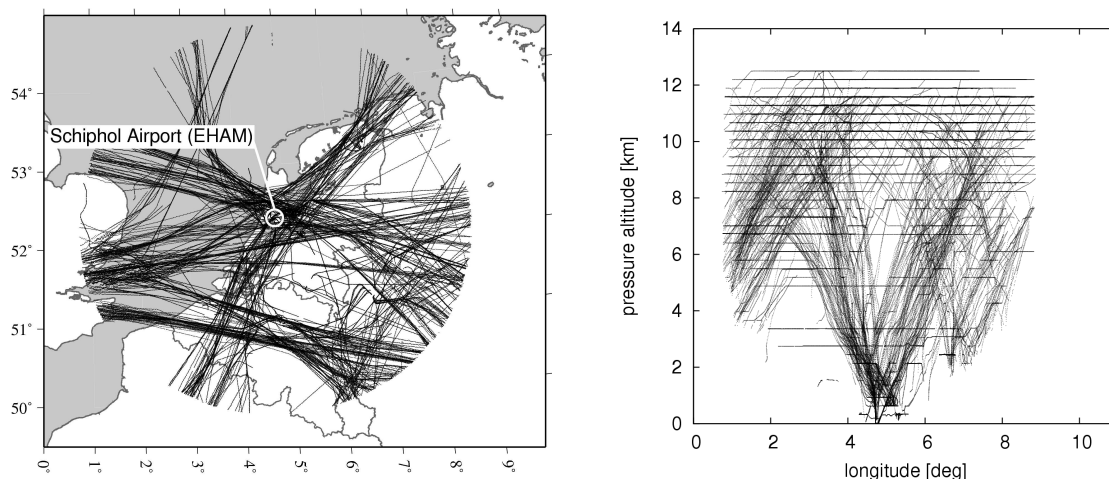


Figure 2.1: Horizontal and vertical coverage of ModeS data on 2008-03-13 from 11:00 UTC to 13:00 UTC.

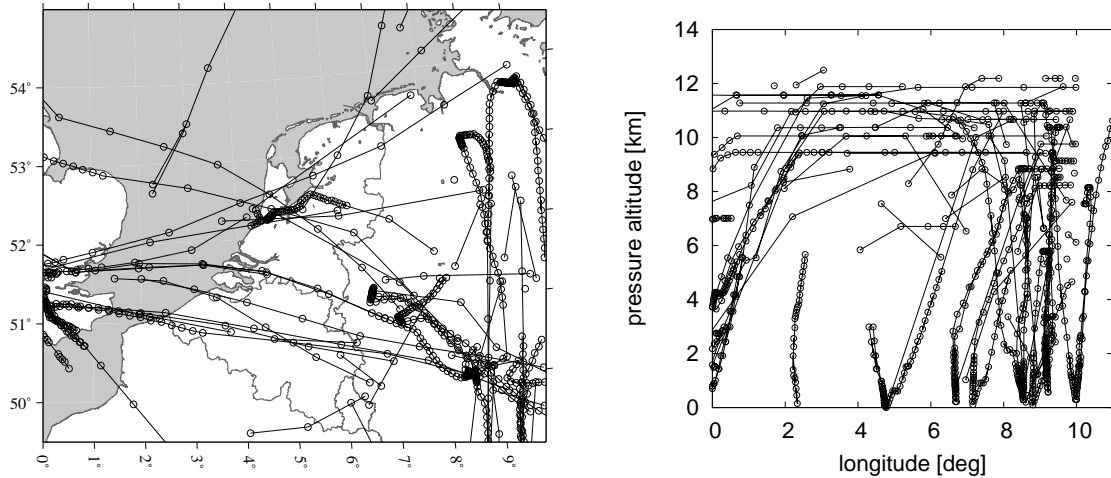


Figure 2.2: Horizontal and vertical coverage of AMDAR data on 2008-03-13 from 11:00 UTC to 13:00 UTC.

2.2 AMDAR

Aircraft are equipped with instruments to measure temperature and to derive wind. At present, a selection of these observations are transmitted to a ground station using the AMDAR (Aircraft Meteorological Data Relay) system. An atmospheric profile can be generated when measurements are taken during takeoff and landing. See WMO (2003) for more details. The coverage of this data on 2008-03-13 from 11:00 UTC to 13:00 UTC is shown in Figure 2.2.

AMDAR uses raw data available from the aircraft monitoring systems. Data rates typically vary from one sample per second to 16 samples per second. According to WMO (2003) to reduce the noise, the AMDAR reports are averages of observations over a certain time depending on the phase of flight. This averaging is done internally by the aircraft computer before transmitting the data with averaging times for ascent and descent of 10s and for level flight above flight level FL200 (20 000 ft) of 30s.

The availability of AMDAR data depends on the phase of flight. For level flight an observation frequency is usually once every 7 minutes. In case of a “maximum wind event” an extra observation is made. For an ascending aircraft, observations are made at nine intervals of 10 hPa (or 19 intervals of 5 hPa), followed by pressure observation interval of 50 hPa (or 25 hPa) until a height of 20 000ft is reached (FL200). For a descending plane, the first observation is made at 500hPa, pressure intervals are set to 50hPa (or optionally 25 hPa) until 700 hPa is reached. From 700hPa onwards the pressure observation interval is set to 10hPa (or 5 hPa), see WMO (2003) for the details. The different phases of flight are easily detected in Figure 2.2.

2.3 Radiosonde

In the Netherlands, for more than 50 years radiosonde have been used daily to observe upper air wind, temperature and humidity. The locations where radiosonde are launched globally are

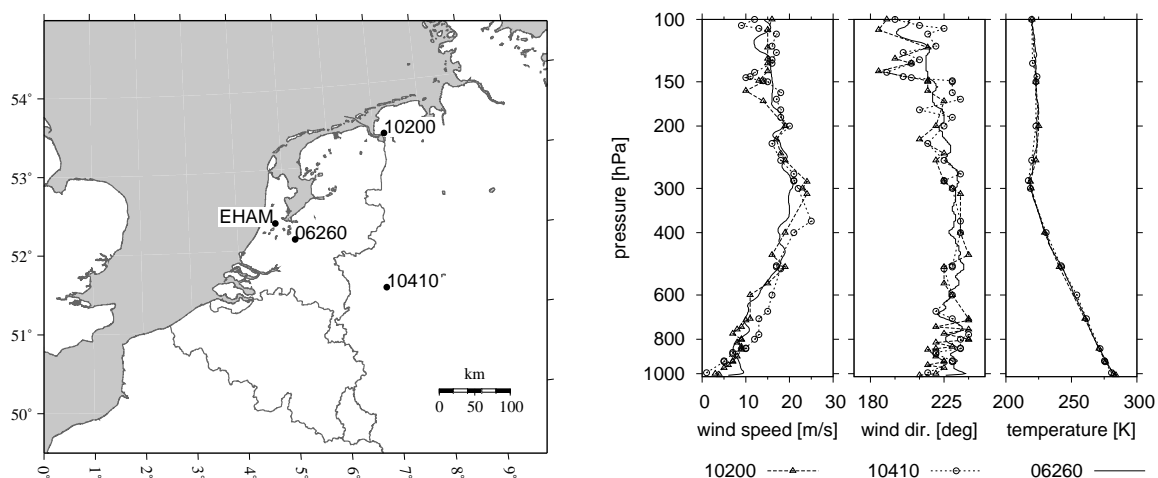


Figure 2.3: Left panel: location of radiosonde launch sites in the neighborhood of the Netherlands. Right panel: vertical profile of the three radiosondes observed of 2008/03/13 12 UTC. Note the difference in profile resolution: 06260 has 536 observations, 10200 has 40 and 10410 has 65 observations.

mainly on land, although there are a number of automatic radiosonde systems on ships (ASAP) and on a few offshore platforms. A radiosonde system consists of a ground segment and a balloon to which a small lightweight container is attached. A temperature sensor and humidity sensor are attached to the container. A calibrated pressure sensor and/or a GPS receiver is used to determine the geopotential altitude (and latitude and longitude position in case a GPS is used). The pressure, temperature and humidity information is transmitted to the ground segment where the wind speed and direction are inferred from the ground track of the balloon during its ascent (using LORAN-C or GPS). The radiosonde is launched approximately 40-50 minutes before the synoptic hour (which are 00, 06, 12 and 18 UTC) to assure that it reaches the tropopause (i.e. 500 hPa) around the synoptic main hour. Furthermore, the equipment is single used and relative expensive. Because of the long duration of the flight, this observation method implies that the actual observation time at a certain height does not correspond to one single timestamp. Because of the wind the radiosonde drifts away, the observed profile does not correspond exactly to the profile above the launch site.

KNMI started radiosonde observations in 1947; currently Vaisala RS92 radiosonde are launched at the main synoptic hours (00 and 12 UTC). This radiosonde has target required measurement uncertainties of 0.1°C for temperature, 0.2 hPa for pressure and 2% for relative humidity.

The distribution of the radiosonde network in Europe is too coarse for meso-scale modeling. Moreover, the frequency of a large number of radiosonde launches in Europe were reduced from four times per day to two in order to reduce the costs of the total meteorological observing network. Despite the coarse temporal and horizontal resolution, radiosonde observations are a valuable source of information on temperature, humidity, and wind in the atmosphere. Figure 2.3 shows the radiosonde launch sites from which observation are used in this study with distance of about 150 to 200 km. On the right a profile valid for 2008-03-13 12 UTC is

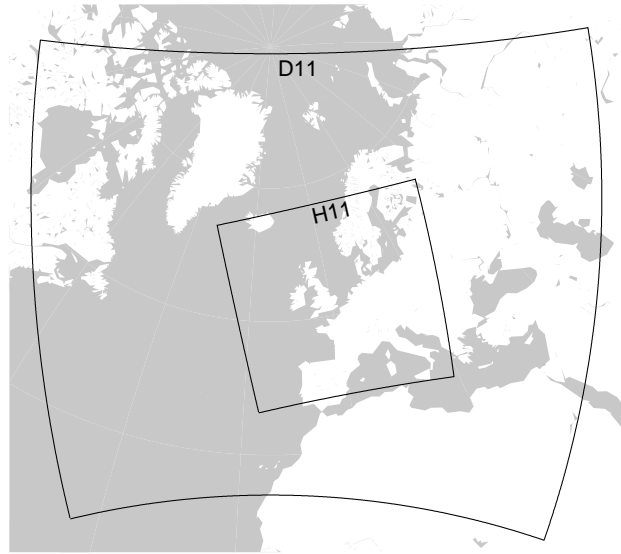


Figure 2.4: NWP model area of H11 and D11.

shown. For observations from De Bilt (06260), 10 second data is available, while for the other two radiosonde only a reduced (so-called TEMP) profile is present. Note that the temperature profiles, for this observation time, are almost equal while the wind profile shows more variation. This is due to the different meteorological scales of temperature and wind.

2.4 Numerical Weather Prediction

Numerical weather prediction (NWP) models can be used to assess the quality and accuracy of (new) observation types. Assimilation of observations into NWP models tends to find the best possible initial state of the atmosphere given the observations, a certain initial guess (also called background or first guess) and constraints. From this initial state a forecast can be computed through integration in time. By comparing different observation types with a NWP forecast an assessment can be made of the quality of the observations in relation to the NWP model. Note that the observed difference includes also model error.

At KNMI a High Resolution Limited Area NWP Model (HIRLAM, Undén et al. (2002)) is run operationally. This model runs every three hours (called H11) or six hours (called D11) and has a forecast length of 24 hours and 48 hours respectively. Both model-runs have a horizontal resolution of 11 kilometers and 40 vertical levels, ranging from the surface to 0.1 hPa. For both models, synoptic observations, such as wind, temperature and humidity from radiosonde and AMDAR and surface pressure observations, are used to analyze the initial state of the atmosphere. A three hour forecast of the previous H11-run is used as background information of the next run. Because the model is a limited area model, the forecast at the boundaries of the region is fixed to the forecasts from the larger HIRLAM D11-run (which has a six hour cycle). The latter six hour cycle is embedded in global forecast fields from the European Centre for Medium Range Weather Forecasting. Figure 2.4 shows the two NWP-regions used.

Chapter 3

Meteorological Observations from Aircraft

Aircrafts are equipped with a large number of sensors for flight management. Some of these sensors measure atmospheric variables, or deliver atmospheric parameters. Systems like ModeS and AMDAR use this data source to obtain upper air wind and temperature. The method of deducing wind information is equal for both systems. AMDAR wind information is retrieved from the pitot-tube observation of static pressure in combination with the ground position, see WMO (2003). For air temperature the method is different: AMDAR provides air temperature from the in-situ measurement by a temperature sensor, while it is inferred from other aircraft parameters for ModeS.

3.1 Observations of Temperature and Wind

ModeS reports information for each aircraft tracked by the radar on: flight level (F) Mach-number (M), roll, true airspeed (V_t or TAS), heading (α_t), groundspeed (V_g) and track angle (α_g). Other information is available, like inertial vertical velocity, but these are not relevant for the current study.

The temperature can be deduced from the true air speed V_t and M using the relation between the speed of sound and temperature and the ideal gas law,

$$M = \frac{V_t}{c}, \quad (3.1)$$

where V_t is in m/s, $c = \sqrt{\gamma R_d T}$ in m/s, $R_d = 287.0528742 \text{ J kg}^{-1} \text{ K}^{-1}$, and $\gamma = c_p/c_v = 1.397774$ is the ratio of specific heats. Thus, given M and V_t , the air temperature T can be calculated by

$$T = 2.4923 \cdot 10^{-3} \frac{V_t^2}{M^2}, \quad (3.2)$$

where T is in K. The Mach-number M has no dimension.

The wind vector \mathbf{V} is obtained from the difference in heading vector, defined by length V_t and angle α_t , and the ground track vector, defined by length V_g and angle α_g , that is

$$\mathbf{V} = \mathbf{V}_g - \mathbf{V}_t \quad (3.3)$$

Flight level is determined using the International Standard Atmosphere (ISA) relationship between pressure and pressure altitude. The temperature as a function of pressure altitude for the ISA is defined as

$$T = T_0 - \Gamma h, \quad (3.4)$$

where h is pressure altitude in meters, $T_0 = 288.15$ K and Γ is the temperature lapse rate of the International Standard Atmosphere, that is $\Gamma = 0.0065$ K m⁻¹. The relation between pressure altitude h (or flight level F , which is related to pressure altitude through $h = 30.48 F$) and pressure p is defined, according to WMO (2003),

$$\begin{aligned} p(h) &= p_0 \left(\frac{T_0 - \Gamma h}{T_0} \right)^{g/(\Gamma R_d)} \quad \text{for } h \leq 11\,000\text{m}, \\ p(h) &= p_1 \exp\left(\frac{-g(h - 11000)}{R_d 216.65} \right) \quad \text{for } h > 11\,000\text{m} \end{aligned} \quad (3.5)$$

where $g = 9.80665$ m/s² and $p_0 = 1013.25$ hPa and $p_1 = 226.3204059$ hPa is the pressure of the International Standard Atmosphere at sea level and 11 km, respectively.

3.2 Air density and airspeed

The focus of this report is on wind and temperature observations; the uncertainty of air density is therefore not assessed. However, the air density and its relation to airspeed is important for flight control and is therefore discussed briefly.

Indicated airspeed (IAS) is the airspeed at ISA mean sea level which represents the same dynamic pressure as that flying at the true airspeed (TAS) at flight level. The relation between the IAS and TAS is, according to Ruijgrok (1990),

$$\text{IAS} = \text{TAS} \cdot f(p, M) \cdot \sqrt{\frac{\rho}{\rho_0}}, \quad (3.6)$$

where

$$f(p, M) = 1 + \frac{1}{8} \left(1 - \frac{p}{p_0} \right) M^2 + \frac{3}{640} \left(1 - 10 \frac{p}{p_0} + 9 \frac{p^2}{p_0^2} \right) M^4, \quad (3.7)$$

and $\rho_0 = 1.225$, the air density at mean sea level in the standard atmosphere. The last equation is an approximation where it is used that $\gamma = 1.4$ and higher order terms are discarded.

At sea level ($p = p_0$) IAS is the same as true airspeed. Knowing the TAS, M and IAS, the air density ratio can be determined:

$$\frac{\rho}{\rho_0} = \frac{\text{IAS}^2}{f(p, M)^2 \text{TAS}^2} \quad (3.8)$$

3.3 Quality control

Based on the mechanical properties of the aircraft and on possible errors in data transmission a number of checks has been proposed by Vegter (2007a,b); Vonk (2008). The checks are given in Table 3.1. Transmission errors may result in negative Mach-number or heading. Airborne aircraft generally have a groundspeed larger than 25 m/s (50 kt) and smaller than 425 m/s (850 kt). A similar range can be found for the true air speed. Because the groundspeed and wind speed in general differ at least an order of magnitude, the heading and the ground track angle difference is within 45 degrees. During manoeuvres, the airflow around the pitot-tube can be irregular and thus observations with a large roll should be omitted.

Table 3.1: Raw ModeS data quality checks.

description	threshold
realistic heading	$\alpha_t \geq 0$
realistic Mach-number	$M > 0$
realistic groundspeed	$25 \text{ m/s} < V_g < 425 \text{ m/s}$
realistic true air speed	$50 \text{ m/s} < V_t < 295 \text{ m/s}$
difference between heading and ground track	$-45^\circ < \alpha_t - \alpha_g < 45^\circ \text{ deg}$
realistic temperature	$T < 370 \text{ K}$
omit large roll	$r < 2.5^\circ \text{ deg}$

Chapter 4

Preprocessing ModeS Observations

4.1 Preprocessing ModeS Temperature Observations

ModeS data is raw data from the internal aircraft computers. Although internally possibly more samples are available, no averaging is applied and a ModeS observation is thus less smooth than an AMDAR observation. Nevertheless, the high observation frequency of once every four seconds can be used for improvements.

The reported resolution of the ModeS data elements is given in Table 4.1. This resolution determines the quality and the accuracy of the inferred meteorological parameters. The resolution of temperature is derived from the resolution M and V_t , through Equation 3.2. An estimate of the error of T is

$$\Delta T = 2.4923 \cdot 10^{-3} \left(2V_t M^{-2} \Delta V_t + 2V_t^2 M^{-3} \Delta M \right), \quad (4.1)$$

which is for $M = 0.7$, $V_t = 200$ m/s around 2-5 K, where the error in M and V_t are taken to be half the resolution. This implies that using the reported values of M and V_t , the temperature may show rapid fluctuations of this order due to the resolution of M and V_t . In Figure 4.1 the distribution of the difference between two successive (i.e. four second difference) observations in temperature and wind for a single day is shown. The rather unrealistic distribution is due to the reported resolution of M and V_t and can be explained by Equation 4.1. Regular temperature jumps of the order of 2 K in four seconds are observed at FL425. For lower flight

Table 4.1: Resolution of the essential elements in the ModeS reports.

element	resolution
latitude/longitude	10^{-4} deg
flight level	0.25 (100ft or 7.62 m)
ground speed/true airspeed	2 kt (or 1 m/s)
track angle/heading angle	≈ 0.1757 deg
Mach-number	0.004

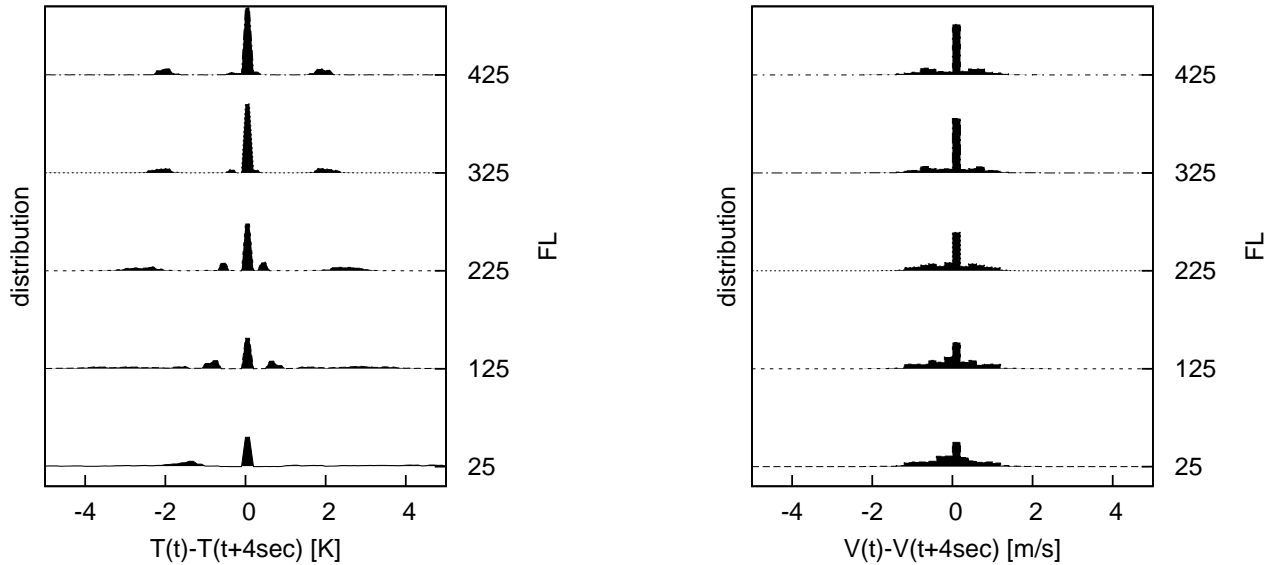


Figure 4.1: Distribution of the difference between two successive raw temperature and wind observations for a single day with respect to the flight level.

levels these differences increase and are more spread. Jumps in wind speed are also observed with a magnitude of 0.5 m/s at FL425 down to 1 to 1.5 m/s at FL25.

A smoothing algorithm is applied to the raw data to deal with this problem. The reports of M and V_t are linearly fitted over a time window. The values of the linear fit of M and V_t in the center of the window is used to calculate T (according to Eq. 3.2). For level flight a window of 60 seconds (15 observations), and for ascending/descending aircraft a window of 12 seconds (3 observations) is used. As stated, the temperature itself is not smoothed but the temperature is re-calculated from the smooth estimates of M and V_t . Additionally, the atmospheric observations are averaged based on similar time intervals as AMDAR: 10 seconds for ascending/descending flight phase and 60 seconds for level flight.

The effect of this smoothing algorithm is shown in Figure 4.2. Clearly, the jumps in temperature and wind speed have disappeared and the distributions have are more Gaussian, which is due to the smoothing and averaging of the temperature and wind observations. Given a speed of 900km/h of the aircraft at FL425, the distance between successive measurements is approximately 1 km. The temperature is clearly less variable at this level than e.g. at FL125. There is also an effect of ascending and descending, especially in temperature due to the difference in vertical velocity. This will result in a skew distribution, which needs further investigation, especially when compared to NWP and the atmospheric resolution resolved. Note that the wind speed difference distribution is rather independent of flight level.

Figure 4.3 shows the raw and smoothed profile for a single aircraft. The left panel shows the raw temperature, M and V_t profile. Clearly visible are the jumps in temperature due to the reported resolution of M and V_t . In the right panel the smoothed profile is shown. The dots are the observations that passed quality control (see Section 3.3).

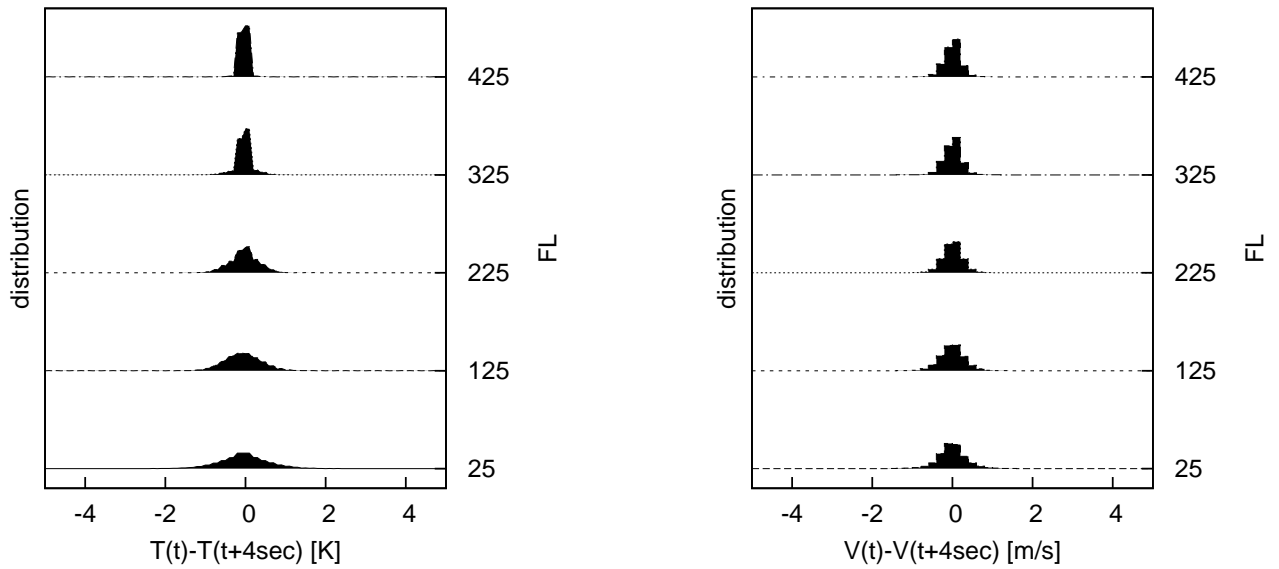


Figure 4.2: Distribution of the difference between two successive smoothed temperature and wind observations for a single day with respect to the flight level.

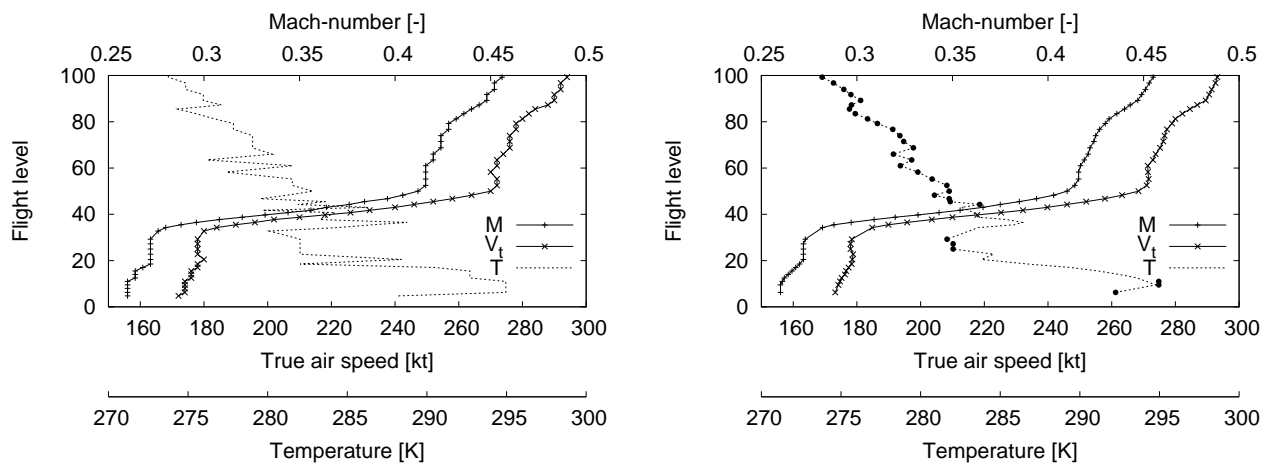


Figure 4.3: Left panel: raw reports of M and V_t , and corresponding T . Right panel: smooth M and V_t and corresponding T (line) and T after quality control (dots).

4.2 Preprocessing Wind Observations

Accurate values of true air speed (V_t) and heading α_t are essential for accurate wind determination. At low wind speeds, errors in V_t and/or α_t can lead to large errors in wind direction, however, systematic errors in α_t are more essential. Investigation on the accurateness of the heading is therefore important and, as it turns out, a calibration of the heading is necessary and feasible in most cases.

4.2.1 Magnetic Heading correction

In the ModeS message, the reported heading is given with respect to the magnetic north. A correction is applied to α_t using the International Geomagnetic Reference Field (Maus and Macmillan, 2005). In Figure 4.4 this field is shown in the vicinity of the Netherlands on 2007-01-01. Currently, the magnetic correction around Schiphol is close to zero. The heading when corrected with the magnetic correction, will be a true north angle.

4.2.2 Heading Correction

A correct heading (with respect to true north) is essential in calculating the wind. It appeared that the magnetic correction is insufficient and that an additional correction is needed. This was already observed by Vegter (2007a) for some aircraft; a heading error of several degrees was reported.

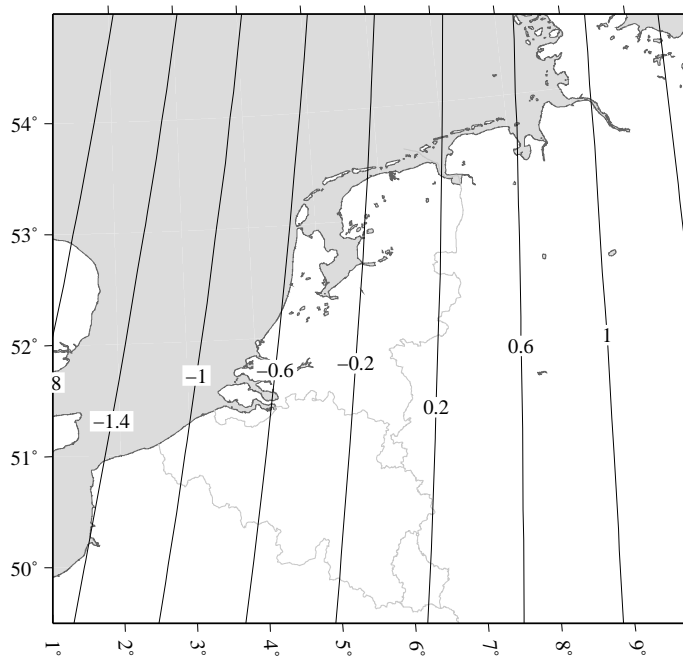


Figure 4.4: Magnetic Reference Field valid for 2007-01-01.

The size of the correction can be detected by inspecting the heading of the aircraft when it (just) has landed on the runway. In this case the heading and runway angle should match (within measurement accuracy). As an example, Figure 4.5 shows the heading and flight level of a Boeing B767-322 (landing at Schiphol airport) versus the ground speed V_g . We may say that when the ground speed is lower than 120 kt and the height is constant the aircraft is on the runway. The offset with the runway angle, when the aircraft has landed, is around 3 degrees in Figure 4.5. Although this is an extreme example, offsets of the order of 1 to 2 degrees are not uncommon.

For a 12 month period the heading corrections are determined for all landing aircraft. The method of detection requires that the position of the aircraft is on the runway, the groundspeed of the aircraft is between 55 and 120 kt and the aircraft has constant “flight level” (of -5 in the example above). At least three data points should meet these criteria in order to store the mean difference between the heading and the runway angle. For aircraft with more than 10 separate landings the mean heading offset and the total standard deviations of the offset is presented in Figure 4.6. The heading offsets are ordered by aircraft type and mean heading offset. The aircraft type are obtained from an internet aircraft database (Kloth, 2009). Some aircraft have very small heading offsets, while others have large offsets and also the standard deviations differs with aircraft type. The new Boeing B772 and B773 and new Airbus A332, A333 and A343, have very small standard deviation values, while older Boeing, like the B733, show to have a large standard deviation in the heading correction.

The change of heading offset with time varies per aircraft type. Some aircraft types have almost no variation, while other types show a large variation. To show that these offsets are not constant over time, the mean offsets per landing are shown in Figure 4.7 for four aircraft over a

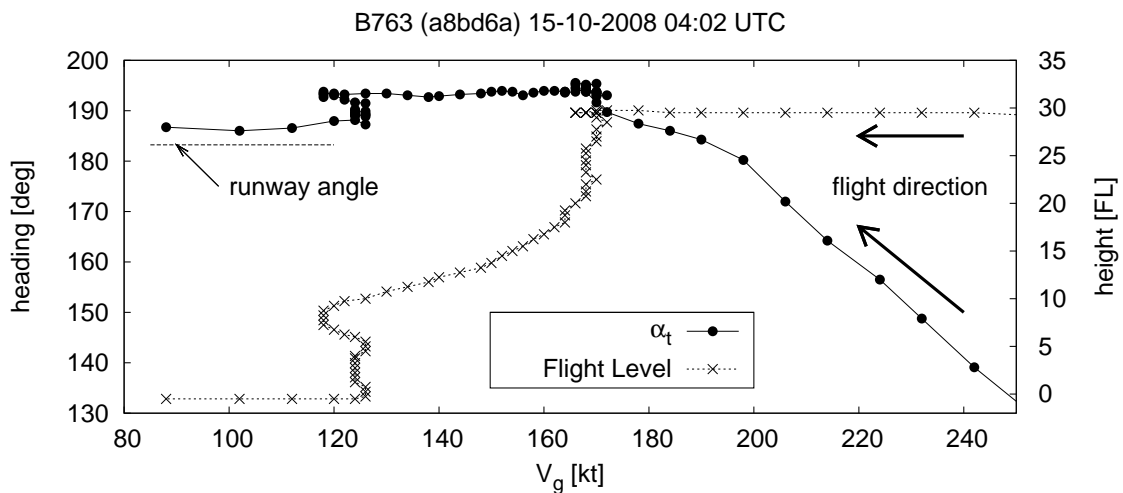


Figure 4.5: Flight data from a Boeing B767-322. The heading with respect to the ground speed is shown by dots; the flight level is shown by crosses. Time runs roughly from right to left, with the last four points showing the landing of the aircraft. The thick arrows indicate the flight direction of the aircraft.

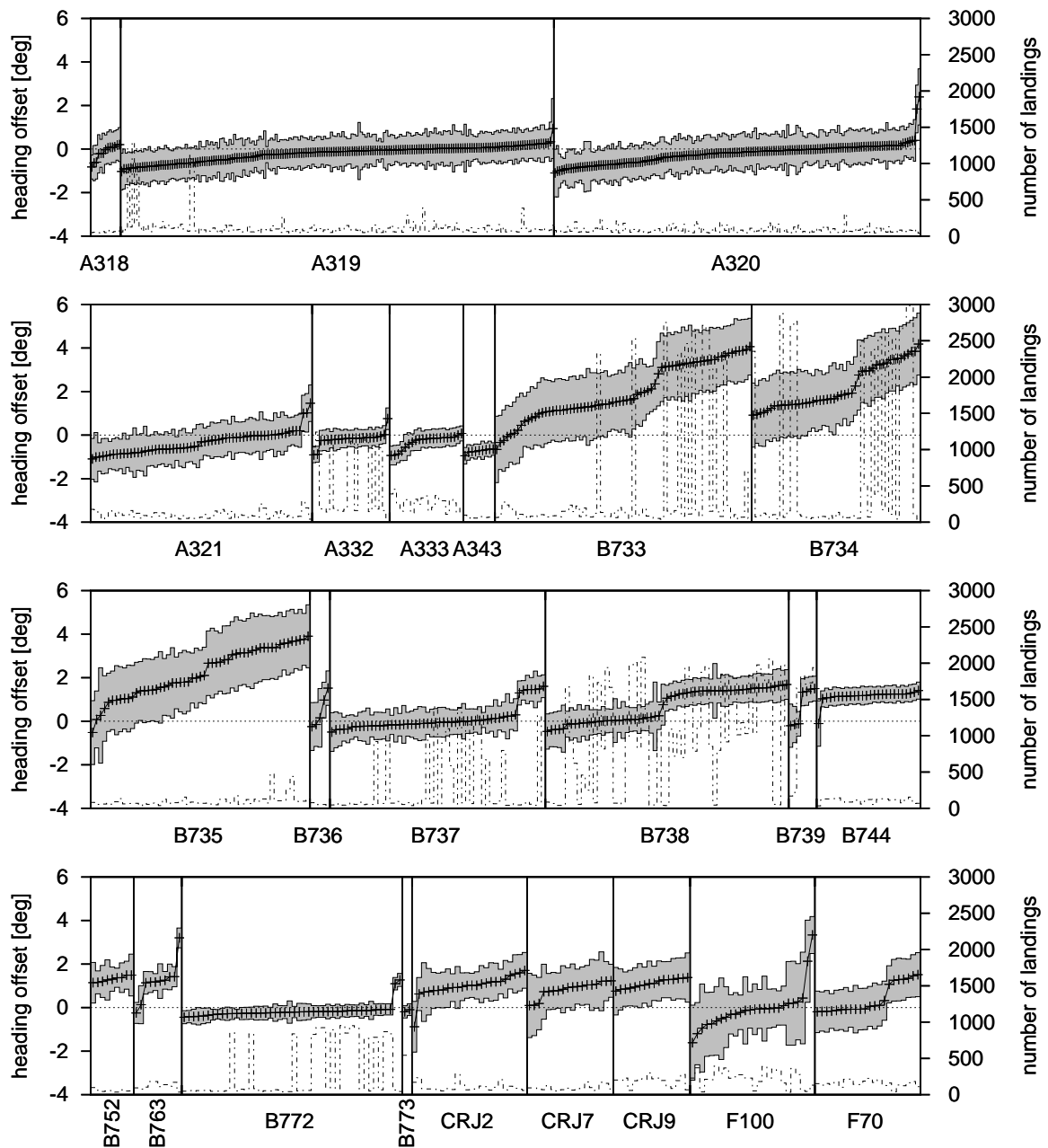


Figure 4.6: Mean and standard deviation of the heading offset for each transponder-id separately. The data is ordered with respect to aircraft type and mean heading offset. Also shown on the right scale is the number of landings for the specific aircraft.

12 month period (top four panels). In the bottom panel, the heading offset of an aircraft with stable heading calibration is shown. The small panels to the right of the large panels depicts the distribution of the offset. Clearly, the two B733 show to have a bi-modal behavior (albeit that the 4840f5 has a less convincing second mode), while both B738 have single heading offset with a large spread. The B772 shows to have a very sharp distribution. Reasons for the bi-modal

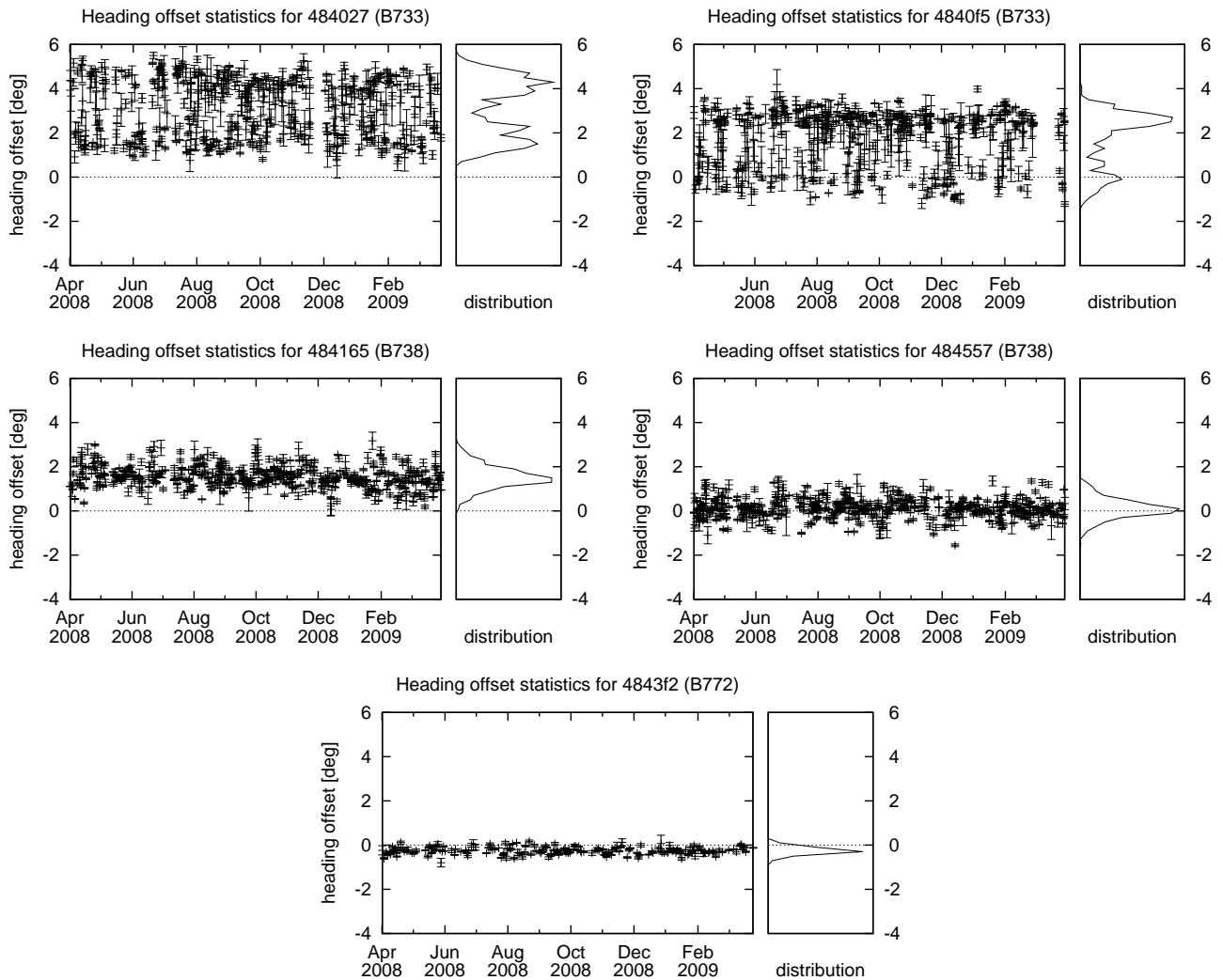


Figure 4.7: Heading offset of five different aircraft. Top two panels are B733, two panels in the middle are B738 and bottom panel is a B772. The small sub-panels on right of each panel shows the distribution of the mean heading offset of each landing. The small error-bar is the standard deviation of the observed offset of each landing separately.

signature could be related to switching between sensors.

The correction applied to the heading is chosen to be the mean offset as shown in Figure 4.6 (crosses). Although, a more sophisticated correction could be applied (i.e. making use of the bi-modal signature), here this first order approach is applied.

Another important note to make is that the reported heading could change after maintenance of the aircraft. However, in the 12 month period we did not see sudden jumps in the heading offset of an aircraft.

Chapter 5

Validation of ModeS

In this chapter the ModeS wind and temperature are validated against NWP, AMDAR and radiosonde observations. The effect of smoothing algorithm and the different heading corrections is first shown by a triple comparison with ModeS, AMDAR and NWP. Next, all ModeS data over a 12 months period is analyzed by comparison with NWP. The last two parts of this section contains a (triple) collocation of ModeS, NWP and radiosonde.

5.1 Triple comparison AMDAR, ModeS and NWP

Over a period of 12 months (March 2008-February 2009) a triple collocation comparison of ModeS, AMDAR and HIRLAM is performed. The HIRLAM data is from a H11-run with at least a forecast time of two hours to avoid that AMDAR information used in the collocation has been assimilated. The hourly NWP forecast fields are linearly interpolated to the observation time. For the observation height a logarithmic interpolation of the pressure is applied.

The ModeS data set is scanned for matching AMDAR observations. When a possible match is found the distance in time and space is used to determine whether the match is good; a minimal number of close observations is required. Hence a lookup table is constructed based on a 12 month dataset. Figure 5.1 shows an example of the collocation of AMDAR and ModeS (position, height, temperature and wind speed). Note that the AMDAR reports (in this case) between FL275 and FL375 are only collected around 16:45, while the observations at 18:30 (ascending) are not present. Note also the significant difference in the reporting frequency between ModeS and AMDAR reports. Also, ModeS observations show a large increase in wind speed at FL300 around 18:30 UTC not observed by AMDAR.

Table 5.1 shows the aircraft types for which a heading correction was available and a collocation with AMDAR was made. Also shown are the number of observations excluded from the comparison due to a gross error check; temperature difference between model and observation were larger than 10 K and/or wind speed differences were larger than 15 m/s. Nearly half of the triple collocated observations stem from B733 and B735. These aircraft have a large uncertainty in the heading offset (see Fig. 4.7), which may influence the assessment of quality.

AMDAR, NWP and ModeS observations are compared and the mean differences and RMSs are calculated before and after smoothing. The improvement in quality in temperature obser-

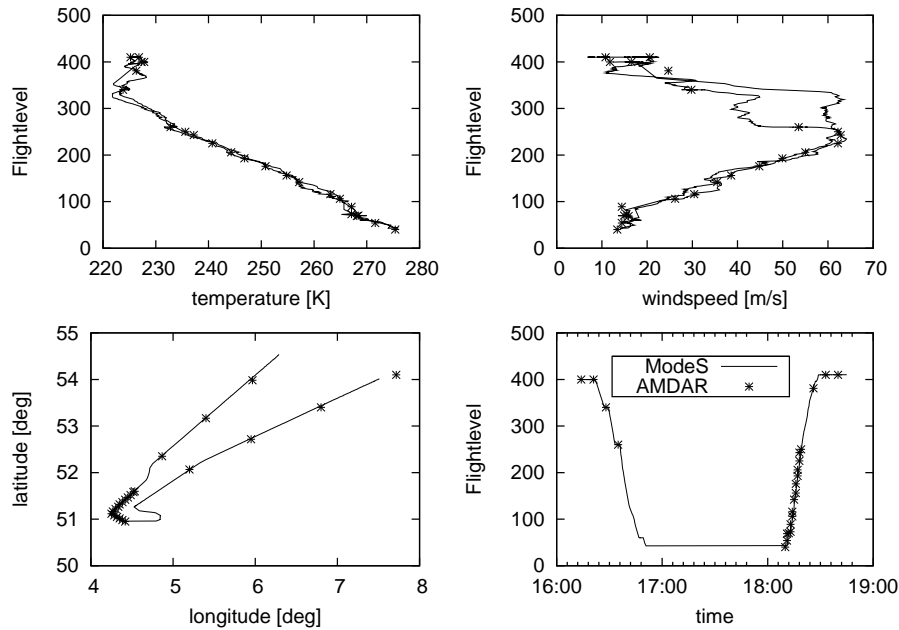


Figure 5.1: Example of a matching ModeS and AMDAR profile.

variations is shown in Figure 5.2. At the lowest levels the effect of the smoothing algorithm is most prominent because at these levels the M and V_t vary the most (due to ascending and descending, causing large temperature changes). At higher levels the impact of the smooth algorithm is smaller, nevertheless a positive impact is observed over the whole profile. Note that the biases do not change (except for the lowest level). The bias between AMDAR and NWP is larger than the bias between ModeS and NWP; both are constant in the upper atmosphere. The RMS of ModeS with NWP is almost twice the RMS of AMDAR due to the resolution of

Table 5.1: Number of triple collocations of ModeS, AMDAR and NWP for different aircraft type. Also shown are the gross error amounts.

model	details	number	observed flights	observations	T and V gross error		
					AMDAR	ModeS	both
A319	A319-114	4	818	4088	1	12	7
	A319-131	1	65	237			
	A319-132	3	198	809	0	3	0
A320	A320-211	4	982	5421	1	22	5
B733	B737-330	19	5354	28255	6	64	17
B735	B737-530	17	4127	23531	11	46	20
B736	B737-683	3	178	1298	0	4	0
B744	B747-406	2	642	6186	0	2	0
CRJ9	CL-600	12	3035	22933	9	25	8
total		65	15399	92758	28	178	57

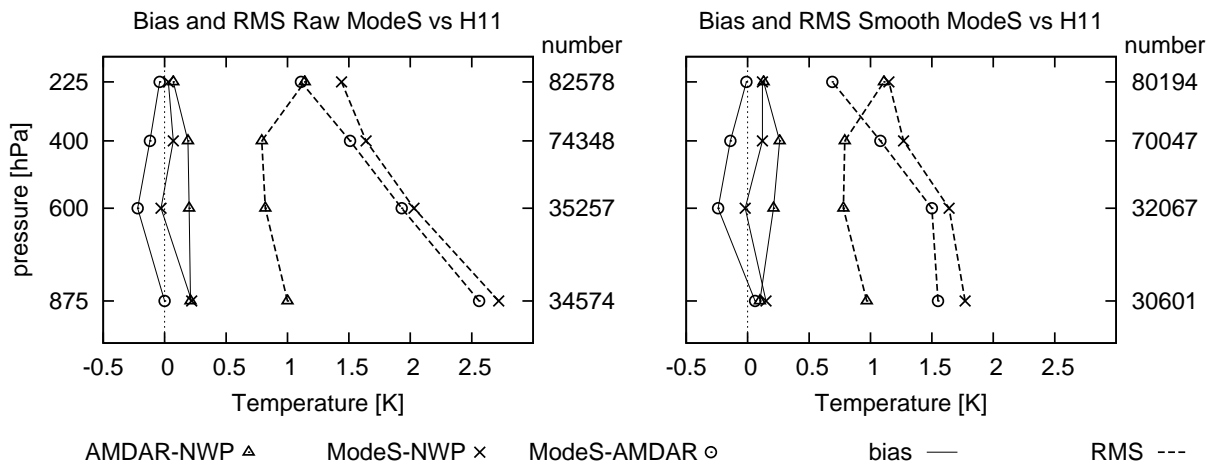


Figure 5.2: Comparison of triple collocations of ModeS, AMDAR and NWP for all AMDAR observations within the range of the tracking radar over a 12 month period.

the reported Mach-number and true air velocity. Note that the smoothing algorithm reduces the number of collocation by 10% in the lower part of the atmosphere and by 5% in the upper part (see the numbers on the right axis of the panels in Fig. 5.2).

Figure 5.3 shows the results of the comparison after applying the heading corrections. When calculating wind direction statistics only observations with wind speeds exceeding 4 m/s are considered. Clearly, applying a magnetic correction has a larger effect on the wind direction statistics, but less on the wind speed. Moreover, the improvement in wind direction RMS is more prominent; the wind direction bias does not show drastic improvements for this correction. The heading correction reduces both the ModeS RMS and bias resulting in an AMDAR-ModeS wind speed RMS of a about 2 m/s. The AMDAR-ModeS RMS in wind speed is smaller than the RMS of both observation systems with NWP. Obviously, both magnetic and heading correction causes useful improvements to the data reducing the bias and RMS. Note that the number of observations in the highest level (FL225) is reduced dramatically. The reason lies in that the heading correction can only be applied to aircraft landing at Schiphol.

For the period March 2008 to February 2009 all ModeS observations are compared to HIRLAM. Figure 5.4 shows the effect of the heading correction for individual aircraft types. For all types the bias and the RMS are reduced. The bias is after the corrections slightly positive with values between -0.2 and 0.5 m/s, and the RMS is reduced to values ranging from 2.5 m/s at the bottom of the profile to 3.5-4 m/s at the top. One outlier in RMS is observed (aircraft type Fokker-100, abbreviated as F100); observations from this type is therefore excluded in forthcoming comparisons.

5.2 Comparison Radiosonde, ModeS and NWP

For the same 12 month period (2008/02-2009/03), comparison is made between radiosonde, ModeS and NWP. Radiosonde observations are collected from three sites: De Bilt (WMO

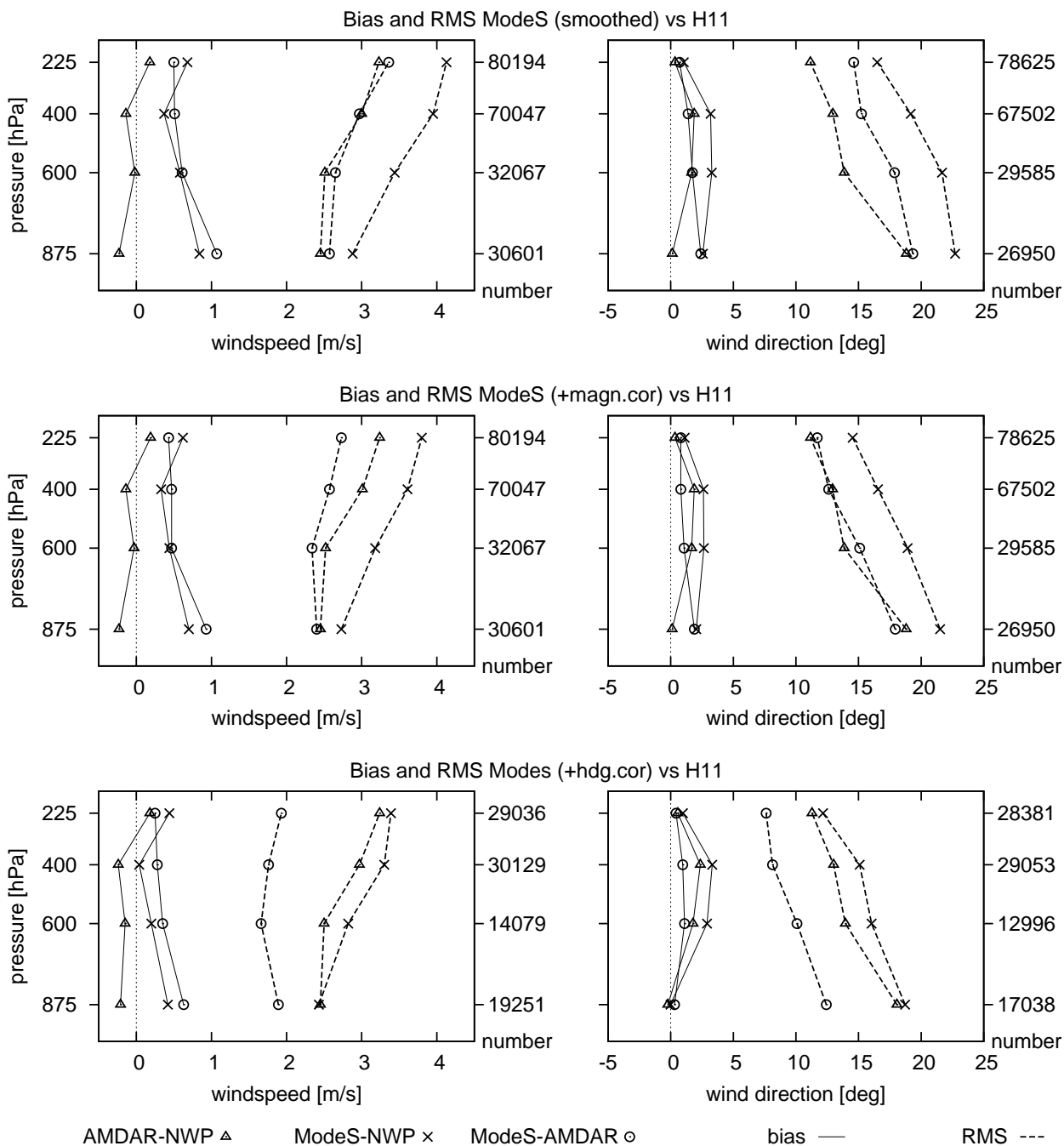


Figure 5.3: Effect on the wind statistics of the corrections applied to the heading by triple collocation of ModeS, AMDAR and NWP. Left panels show the statistics of windspeed; right panels those of wind direction. Top panel shows the statistics using only smoothing. Middle panel shows the statistics of with the additional magnetic correction applied. The statistics shown in the bottom panel are based on all heading corrections.

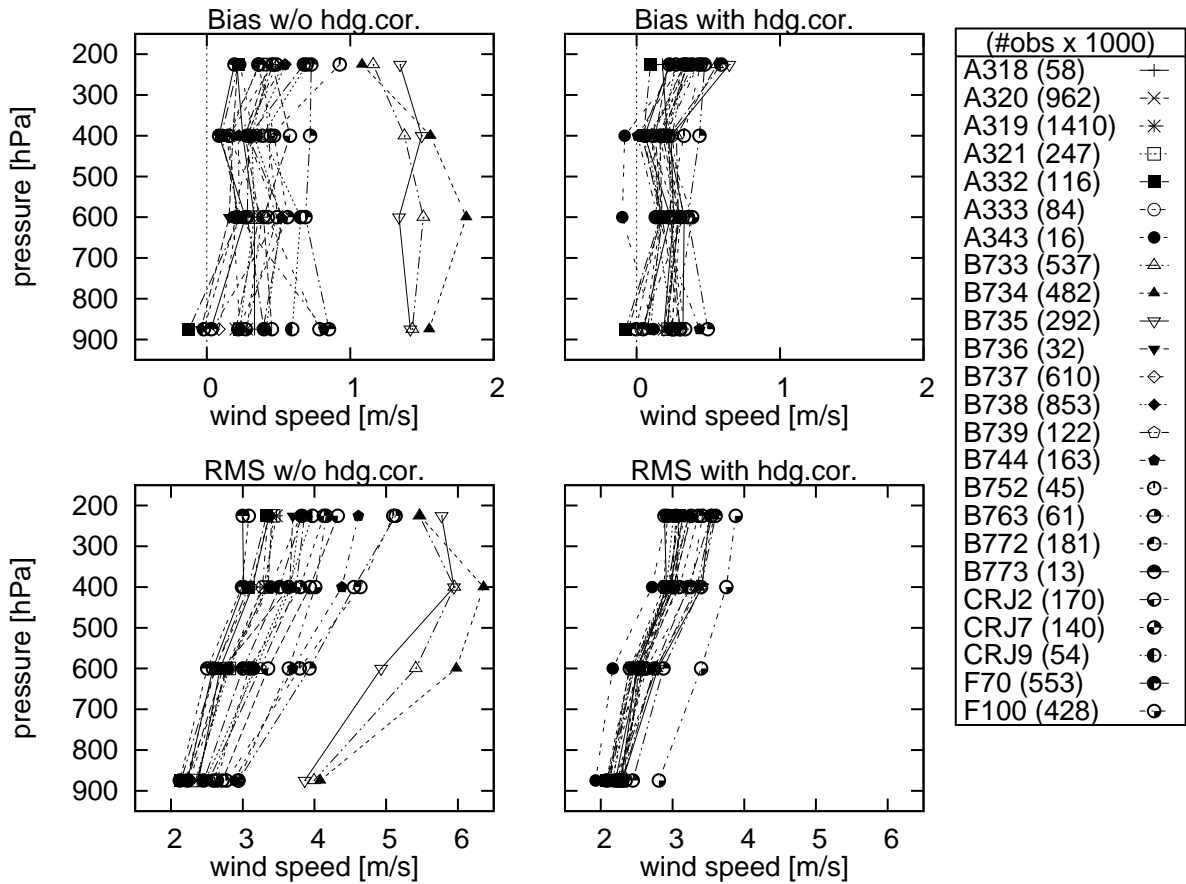


Figure 5.4: Effect of applying the heading correction to all aircraft types. Top panels show the bias before and after correction; bottom panels show the RMS before (left) and after (right) correction.

06260), Emden (WMO 10200) and Essen (WMO 10410). The radiosonde observations from 10200 and 10410 are collected through the international meteorological tele-communication network (GTS). These TEMP observations are reported with a single position, the coordinates of the launch site, and a fixed observation time. For radiosonde observations made in De Bilt, the exact observation time is available because high frequency observations are available. The vertical resolution of the radiosondes also differs: De Bilt has a vertical resolution of approximately 50m, while the other two have a low resolution (only 40-70 observations in a profile, see Figure 2.3).

In Figure 5.5 the statistics for wind speed, direction, u - and v -component and temperature are shown for observations from radiosonde and ModeS. Note that, as before, low wind speed observations (smaller than 4 m/s) are excluded from the wind direction statistics. Table 5.2 presents the total of number of observations per level and per observing system. Also shown in Figure 5.5 are the statistics when compared to the static 06260 profile (abbreviated as 06260(S) and denoted by open boxes), to show the effect of constant horizontal position and time: this

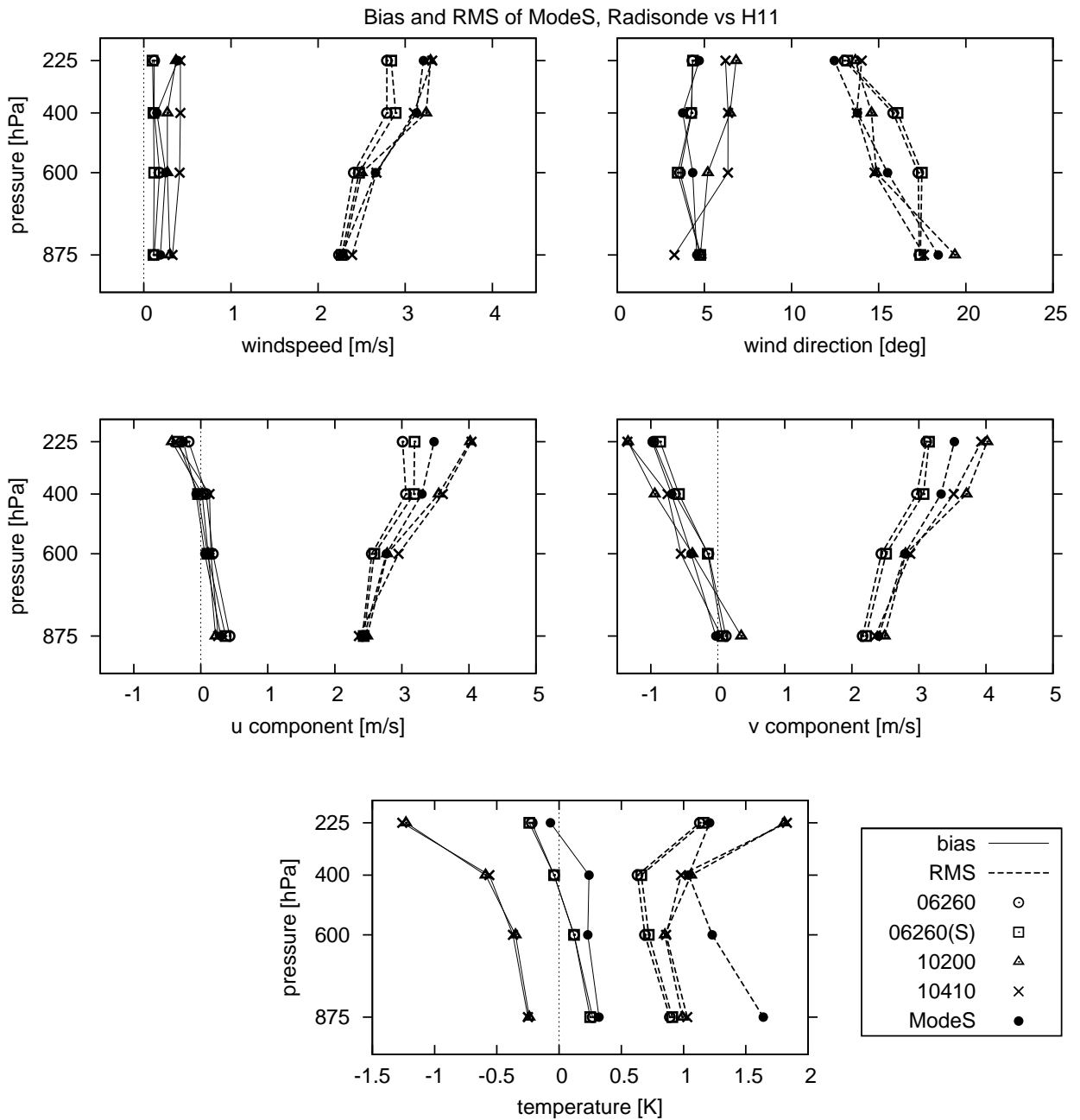


Figure 5.5: Comparison of 12 month of wind and temperature observations from radiosonde and ModeS with HIRLAM.

effect is very small when compared to NWP. For wind speed radiosonde 06260 has the smallest bias and RMS with respect to NWP. For wind direction, both ModeS, 06260 and 10200 have an almost constant zero bias, while the other 10410 has a bias of around +3 degrees (apart from the surface). The RMS for wind direction of 06260 in the center of the profile is typically larger than the other RMSs. The reason for this difference is not clear. The bias u -component

Table 5.2: Number of radiosonde and ModeS temperature and wind observation comparisons shown in Figure 5.5.

p [hPa]	06260		10200		10410		ModeS	
	T,u,v,f	d	T,u,v,f	d	T,u,v,f	d	T,u,v,f	d
875	34603	30609	1892	1679	1351	1184	1745398	1558079
600	31812	29815	1301	1202	1272	1181	1139702	1069459
400	46725	45464	729	706	689	674	1877682	1824157
225	57843	56740	1780	1740	1824	1788	2918555	2858171

is similar for all four observing systems, while the RMS of 06260 is smaller than the others in the top of the profile; ModeS also has a smaller RMS than the other two radiosonde. For the v -component, all observing systems have a (almost) negative bias decreasing with height, with 06260 showing the smallest bias, and 10410 the largest bias. The RMS of 06260 is clearly smaller than the other three. The bias in temperature of 10200 and 10410 is around -1.2 at the top of the profile, while the other radiosonde and ModeS show smaller biases (in absolute value). The RMS of 06260 is the smallest, while ModeS has the largest RMS. Except for the top level, the ModeS statistics are in agreement with those found in the AMDAR-triple collocation comparison.

In general, radiosonde 06260 has the lowest bias for both wind and temperature; ModeS wind observations are of equal or slightly better quality than the radiosonde observations TEMPs from 10200 and 10410.

5.3 Triple collocation of ModeS, NWP and Radiosonde

Note that the dataset shown in the previous section is not triple collocated. Differences in statistics cannot be separated from NWP model forecast problems (due to for example initialization problems). Therefore a triple collocation with 06260 (dynamic position) is made. ModeS observations are collocated with radiosonde observations when the distance between both observations is less than 20km, the difference in height is less than 100ft (30.48m) and the time difference is less than 120 seconds. Because of the high resolution of ModeS observation on average around four ModeS observations are within 100ft and 120 seconds to a single radiosonde observation (for radiosonde observations valid around 12 UTC). The ModeS observations closest in distance to the radiosonde observation is chosen in case of multiple collocation.

In Figure 5.6 the bias and RMS of the triple collocation of ModeS, radiosonde 06260 and NWP is shown. The 400hPa wind (speed, direction, u and v) statistics deviates from Figures 5.3 and 5.5. which can be explained by the reduced number of data points. No seasonal impact was observed. The v -component of radiosonde and ModeS match very well at 400 hPa, while

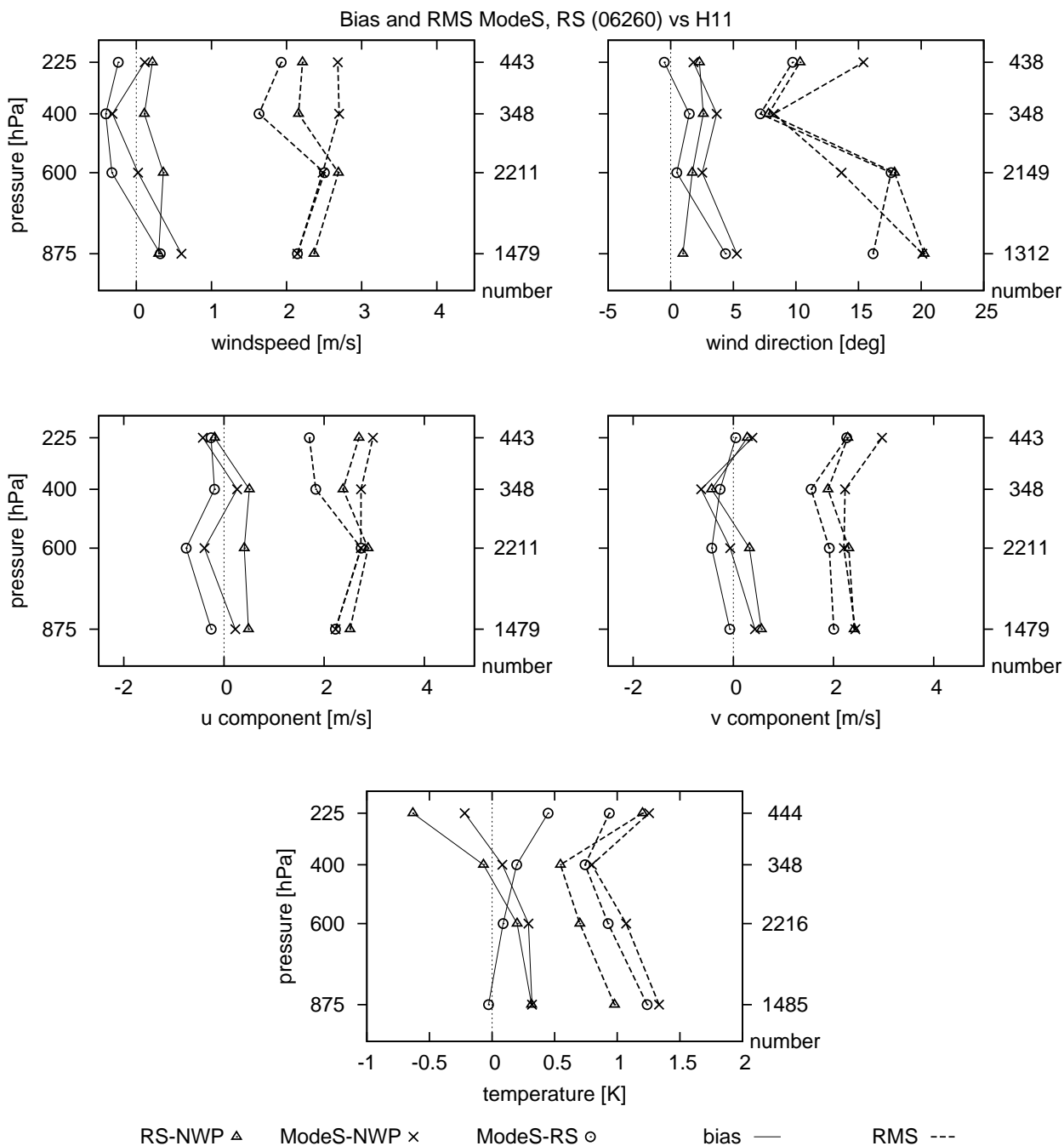


Figure 5.6: Statistics of the triple comparison of wind and temperature using ModeS, radiosonde and NWP. The number used in the comparison is shown on the right axis of each panel.

both observations types compared to NWP show to have large biases and RMS. The NWP model most likely has an anomaly, this needs further investigation. The same signal is present in the *u*-component, although less strong.

The wind speed RMS (top left panel, thick dashed lines) has some agreement with the non-collocated observed values. It appears that radiosonde has a significant and positive wind speed bias with NWP over the whole atmospheric profile, while ModeS has a zero bias to negative at the center of the profile and a positive bias at both the top and the bottom of the profile. Note that this bias for ModeS was not observed for the non-collocated statistics. The wind direction statistics show that in the lower part of the atmosphere the bias is larger than the bias of radiosonde with NWP. Apart from the lowest level, the RMS are close.

For the wind-component statistics, the bias between ModeS and NWP is close to zero (except for 400hPa), and the RMS between radiosonde and ModeS are smaller than those with NWP in the upper atmosphere. In the lower part of the atmosphere this is not the case. The RMS of radiosonde and NWP is larger than the RMS of ModeS and NWP.

The temperature bias of radiosonde with NWP shows to be negative at in the upper part and small (but positive) at the bottom of the profile. The positive bias between ModeS and radiosonde has been observed by Ballish and Kumar (2008) for AMDAR observations. Note that ModeS is a little warmer in the lower part and a little colder in the upper part compared to NWP. The observed RMSs are better than for the ModeS-AMDAR-NWP triple comparison.

The above triple comparison shows that wind speed observations from ModeS and radiosonde have almost similar quality with radiosonde wind performing slightly better. For temperature, ModeS observations are of poorer quality than radiosonde temperature observations.

Chapter 6

Conclusions

In this report the quality of ModeS data is assessed. After a 12 month period comparison between ModeS, AMDAR, radiosonde and numerical weather prediction (NWP) models it is concluded that ModeS wind observations have a quality suitable for assimilation in NWP. This quality is achieved only after pre-processing steps are applied. The required steps are:

- smoothing Mach and true air speed (over 12 for ascending/descending aircraft or 60 seconds level flight)
- averaging wind and temperature observation over 12 or 30 seconds (depending on the phase of flight)
- magnetic heading correction
- aircraft specific heading offset correction

Smoothing is required due to the resolution of the reported Mach-number and airspeed. Magnetic heading correction is necessary to obtain a true north heading reference and an additional aircraft specific heading correction is required to calibrate the heading to the true north. The latter heading correction is determined by collocation of the aircraft when on the runway during landing.

Without the pre-processing steps the ModeS wind speed RMS compared to NWP is 2.5 to 6 m/s, while after applying the steps the wind speed RMS ranges from 2.5 to 4 m/s. The improved wind observations from ModeS are of almost similar quality as AMDAR winds, of equal quality as radiosonde observations from Emden and Essen (Germany), and slightly worse than high resolution radiosonde observations from De Bilt (the Netherlands). ModeS temperature observations are less accurate than AMDAR and radiosonde. The mean difference with NWP is similar to that of AMDAR and radiosonde, the RMS, however, is almost twice as large.

Given the accuracy of the wind from ModeS (after pre-processing) this data is a valuable source of information for meteorology, especially for a meso-scale numerical weather prediction model. The observations frequency can be exploited by setting up a short assimilation cycle

(e.g. one hour) of NWP and produce (in near real-time) an analysis and forecast which could be used for nowcasting applications.

Currently, the heading offset is determined using the data from landing aircraft. This diminishes the number of available observations for pre-processing because not all aircraft observed in the Dutch airspace are landing frequently at Schiphol. Another method to determine the offset could be based in NWP data: using NWP wind the offset of long time series could be examined. In this way, the heading offset of all aircraft frequently visiting the Dutch airspace can be determined and the observations can be used. This method could be valuable and needs further investigation.

Recommendations

Calibration of the heading is necessary. Airlines should be asked to perform a calibration on a regular basis. At this moment it is not known, whether this is feasible.

Acknowledgments

The author would like to thank Peter Oudendijk, Paul de Kraker, Ferdinand Dijkstra and Henry Dwarswaard (all LVNL) and Ad Stoffelen (KNMI) for provision of the data, discussion and helpful comments. Jitze van der Meulen (KNMI) is thanked for carefully reading this manuscript.

This study has been carried out in close cooperation with the Knowledge & Development Centre Mainport Schiphol in The Netherlands (KDC, <http://www.kdc-mainport.nl>).

Bibliography

- Ballish, B. A., and K. V. Kumar, 2008: Systematic Differences in Aircraft and Radiosonde Temperatures, *Bull. Amer. Meteor. Soc.*, **89**, 1689–1707.
- Drüe, C., and W. Frey, and A. Hoff and Th. Hauf, 2007: Aircraft type-specific errors in AMDAR weather reports from commercial aircraft, *Q. J. Roy. Met. Soc.*, **134**, 229–239.
- Kloth, R. D., 2009: Aircraft registration database lookup, *Internet database*, <http://www.airframes.org/>.
- Maus, S., and S. Macmillan, 2005: 10th Generation International Geomagnetic Reference Field, *Eos Trans. AGU*, **86**.
- Ruijgrok, G.J.J., 1990: *Elements of airplane performance*, Delftse University Pers, 452 pp.
- Undén, P., and L. Rontu, and H. Järvinen, and P. Lynch, and J. Calvo, and G. Cats, and J. Cuxart, and K. Eerola, and C. Fortelius, and J. Garcia-Moya, and C. Jones, and G. Lenderlink, and A. McDonald, and R. McGrath, and B. Navascues, and N. Nielsen, and V. Odegaard, and E. Rodriguez, and M. Rummukainen, and R. Rõõm, and K. Sattler, and B. Sass, and H. Savijärvi, and B. Schreur, and R. Sigg, and H. The, and A. Tijm, 2002: HIRLAM-5 scientific documentation, *Technical report*, HIRLAM-project, Norrköping, <http://hirlam.org>.
- Vegter, J. J., 2007a: LVNL Meteo Server - Analysis report MS/S&I/SDI, *Technical report*, Luchtverkeersleiding Nederland.
- Vegter, J. J., 2007b: Onderzoek MS/S&I/SUR - LVNL Meteo Server, *Technical report*, Luchtverkeersleiding Nederland.
- Vonk, B., 2008: First evaluation of high resolution observations from commercial aircrafts, *Student report*, Wageningen University.
- World Meteorological Organization, 2003: WMO AMDAR reference manual, *WMO-no.958*, WMO, Geneva, <http://www.wmo.int>.